

# INTERNATIONAL SOCIETY FOR SOIL MECHANICS AND GEOTECHNICAL ENGINEERING



*This paper was downloaded from the Online Library of the International Society for Soil Mechanics and Geotechnical Engineering (ISSMGE). The library is available here:*

<https://www.issmge.org/publications/online-library>

*This is an open-access database that archives thousands of papers published under the Auspices of the ISSMGE and maintained by the Innovation and Development Committee of ISSMGE.*

# Small-strain shear modulus and shear strength of an unsaturated clayey sand

## Module de cisaillement en petites déformations et la résistance au cisaillement d'un sable argileux non saturé

Georgetti G.B., Vilar O.M.  
University of Sao Paulo, Brazil

Rodrigues R.A.  
Sao Paulo State University, Brazil

**ABSTRACT:** This paper presents and discuss results of laboratory tests with a compacted clayey sand. Two sets of tests were performed to analyze the shear strength and the small-strain shear modulus ( $G_o$ ) of this soil. The first set consisted of triaxial compression tests performed on saturated specimens and multistage triaxial compression tests with controlled suction on unsaturated specimens, which were sheared under constant water content. The second set consisted of tests to measure the  $G_o$  of specimens under constant suction using the bender elements technique. The results allowed observing the development of suction during shearing and influence of suction and confining stress on the shear strength and on the small-strain shear modulus of the tested soil. A planar failure envelope could nicely fit experimental data of shear strength. The influence of net confining stress on the small-strain shear modulus reduced as the suction increases. The shear modulus tended to increase non-linearly with suction, seeming to reach an asymptotic value.

**RÉSUMÉ :** Cet article présente et discute les résultats des essais de laboratoire sur un sable argileux compacté. Deux séries d'essais ont été effectuées pour analyser la résistance au cisaillement et le module de cisaillement en petites déformations ( $G_o$ ) de ce sol. La première série comprenait des essais de compression triaxiaux réalisés sur des échantillons saturés et des essais de compression triaxiale avec succion contrôlée sur des échantillons non saturés, qui ont été cisailés en teneur en eau constante. Les essais de la deuxième série ont servi à mesurer le  $G_o$  d'échantillons sous succion constante en utilisant la technique des *bender* éléments. Les résultats obtenus ont permis l'observation de la succion pendant le cisaillement du sol. Ils ont aussi permis d'observer l'influence de la succion et de la contrainte de confinement sur la résistance au cisaillement et le module de cisaillement du sol testé. Une enveloppe de rupture plane pourrait bien représenter les données expérimentales de résistance au cisaillement. L'influence de la contrainte de confinement sur le module de cisaillement diminue avec l'augmentation de la succion. Le module de cisaillement a tendance à augmenter de façon non linéaire avec succion, semblant atteindre une valeur asymptotique.

**KEYWORDS:** Unsaturated soil, shear modulus, bender elements, shear strength.

### 1 INTRODUCTION

Unsaturated soils are present in large areas worldwide, especially in tropical and subtropical zones. Soil water in unsaturated soil is under suction, which is known to influence the mechanical and hydraulic properties of the soils. For instance, it is known that shear strength increases with suction up to some limit value and that hydraulic conductivity tends to decrease with suction by many orders of magnitude, depending on the level of suction considered. Several laboratory techniques have been developed or adapted to evaluate the suction influence on key properties of the soils, such as the axis translation technique (Hilf 1956) used to control soil suction in triaxial and consolidation tests. In particular, triaxial compression tests on unsaturated samples are used not only to evaluate shear strength but also to estimate soil stiffness through the analyses of stress-strain curves. However, these stiffness measurements face many drawbacks as pointed out by Atkinson and Sallfors (1991). An attempt to overcome such difficulties is using local displacement transducers (Jardine et al. 1984) and bender elements (Dyvik and Madshus 1985) in conventional laboratory apparatuses. Specifically, bender elements technique has increasingly called the attention of researches over the past decades. This technique intends to be a simple and accurate method to measure the small-strain shear modulus of the soil (Dyvik and Madshus 1985). When compared to other methods of obtaining the small-strain shear modulus, bender elements technique provided good agreement or slightly overestimated

values in tests performed by Youn et al. (2008) and Hoyos et al. (2008).

This paper presents test results performed to investigate the shear strength and the shear modulus at small strains of a compacted sandy soil formed under tropical environment. The shear strength was obtained through triaxial compression tests, which were conventional consolidated-drained for saturated soil and constant water content tests for unsaturated soil. The small-strain shear modulus was measured using bender elements in both saturated and unsaturated soil at different suctions and under different isotropic confining pressures.

### 1 SOIL PROPERTIES AND SPECIMENS PREPARATION

The soil used in this investigation is a clayey medium to fine sand of colluvial origin. It was under the action of pedogenetic processes typical of tropical environments, where periods of intense rain and elevated temperature induce severe weathering process. As a result, bases and silica are removed, remaining the more resistant minerals such as quartz. Resulting clay fraction is composed by iron and aluminum oxides and kaolinite. The soil presents liquid and plastic limits of 32 and 16%, respectively. The fine to medium sand fraction is 67% and the clay content is 28%. According to the Unified Soil Classification System it is a SC soil. Standard Proctor parameters are maximum dry density of 1.80 g/cm<sup>3</sup> and optimum water content of 13.8%.

The triaxial compression and bender element tests were performed with dynamically compacted specimens molded with

13.8% of water content and relative compaction of 95% of maximum dry density from Standard Proctor.

The soil-water retention curve for such compaction condition is shown in Figure 1. Plate funnel and filter paper techniques were used to obtain the experimental data on drainage path. The model proposed by Fredlund and Xing (1994) was fitted to experimental data, providing Equation 1 to represent the soil-water retention curve.

$$Sr = 33.6 + \frac{100 - 33.6}{\left[ \ln \left[ e + (\psi / 3.62)^{2.72} \right] \right]^{0.320}} \quad (1)$$

where  $Sr$  is the saturation degree and  $\psi$  is the matric suction.

This is a typical curve of sandy soil, with low air-entry value and large desaturation for suction variation between 4 and 10 kPa. The relative low dry density after compaction also contributes to these features.

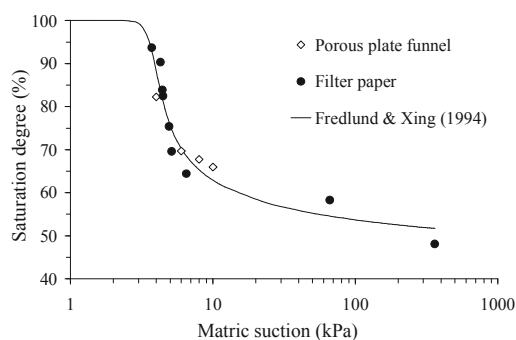


Figure 1. Soil-water retention curve.

## 2 TESTING PROCEDURES

### 2.1 Shear strength

In this experimental program, triaxial compression tests were performed to investigate the shear strength of the soil. The tests comprised shearing five saturated specimens under consolidated-drained (CD) condition. Additionally, three constant water content (CW) triaxial tests were carried out on unsaturated specimens, which were previously led to some known suction. The multistage technique (Ho and Fredlund 1982) was chosen for these latter experiments in order to reduce their duration, as suction equilibrium is a known time consuming process.

In the CD tests, the specimens were saturated by backpressure until the parameter B was at least 0.95. Next, the soil was isotropically consolidated and then sheared at a strain rate of  $10^{-3}\%/s$ , which is lower than the calculated from the consolidation stage. The effective confining pressures were of 50, 100, 150, 300 and 500 kPa.

For the CW tests, the specimens went through a pre-testing procedure, which consisted of reducing the compaction-induced suction to zero by capillary rising, and then imposing target suction via axis translation technique in auxiliary chambers. In the CW tests, the soil was consolidated maintaining constant suction ( $u_a - u_w$ ), where  $u_a$  and  $u_w$  are respectively pore-air and pore-water pressures, and increasing the net confining pressure ( $\sigma_3 - u_a$ ) at each stage. The net confining pressures were of 50, 150, 300 and 500 kPa, and target initial suctions were of 15, 40 and 100 kPa. At the end of consolidation, pore-water pressure was allowed to equilibrate by closing the water drainage valve. Then, suction at the beginning of shearing was computed from the difference between pore-air and water pressures. Maintaining pore-water undrained and pore-air pressure controlled, shearing was carried out at a strain rate of  $6.7 \times 10^{-5}\%/s$  until axial strains of about 5%, where stress

approximately leveled off. In the fourth stage, the specimen was allowed to shear up to larger strains. The strain rate of CW tests was selected based on data of triaxial compression tests on different soils types gathered by Fredlund and Rahardjo (1993) and also on tests presented by Georgetti and Vilar (2010) in the same soil.

### 2.2 Small-strain shear modulus

The experimental program also comprised tests to measure saturated and unsaturated soil shear modulus.

Saturation and suction imposition prior to testing were carried out following the procedure described in 3.1. During the tests, the specimens were consolidated in triaxial cells with bender elements embedded in the top caps and base pedestals. Different levels of isotropic stress were applied keeping saturation or constant suction. This paper focus on part of these experiments in which the soil were confined in steps from 10 to 500 kPa of isotropic effective stress or net stress, for the saturated and unsaturated specimens, respectively. At the end of each confining step, shear waves were transmitted through the soil by the bender elements. Input signals were single sine pulses with a voltage of 14 V and frequencies that ranged from 1 to 50 kHz. Such wide range of frequencies allowed selecting the pulses with minor signal interferences of near-field effects. The small-strain or maximum shear modulus of the soil was then calculated by Equation 2.

$$G_o = \rho V_s^2 \quad \text{with } V_s = L/t \quad (2)$$

where  $\rho$  is the density of the soil;  $V_s$  is the shear wave velocity;  $L$  is the wave path length, taken as the distance between the tips of source and receiver bender elements; and  $t$  is the shear wave travel time.

The shear wave travel time was estimated as the first arrival of the received signal, more specifically, as the time interval between the transmitted and the first major deflection of the received signal. Besides being straightforward, the first arrival has been recommended as a reliable method for calculating the shear velocity (see Chan 2010 and Clayton 2011, for instance).

Four tests were carried out following the above procedure, with suction ranging from zero (saturated soil) to 100 kPa.

## 3 RESULTS AND DISCUSSIONS

### 3.1 Shear strength

From the triaxial compression tests with both saturated and unsaturated soil, the maximum deviator stresses were used to obtain shear strength parameters. It was possible to fit two shear strength envelopes: one, up to approximately 200 kPa of stress and other considering the stresses larger than 200 kPa. The corresponding shear strength parameters were effective cohesion ( $c'$ ) = 10 kPa and effective friction angle ( $\phi'$ ) =  $31^\circ$ , and  $c' = 0$  and  $\phi' = 33^\circ$ , respectively.

Regarding constant water content triaxial compression tests in the unsaturated compacted soil, typical stress-strain and suction-strain curves are shown in Figures 2 and 3, respectively. Figure 2 shows that shear strength increased at each stage and small elastic strains were recovered when the specimen was axially unloaded to beginning the next stage of testing. The visual inspection of specimens and the format of the stress-strain curves indicate that no distinct failure plane was formed and therefore is reasonable to use the multistage test to evaluate the shear strength of this soil. Figure 3 reinforces a tendency of suction variation that was already observed by Georgetti and Vilar (2010): after an initial decrease, suction tended to increase for the lower net confining stresses and remained approximately constant for the larger confining stresses. Rahardjo et al. (2004)

also noticed suction reduction for axial strains until about 3% and smaller changes as shearing progressed after that. The authors performed CW tests on a compacted residual soil from the Jurong sedimentary formation using a suction range that is above the range chosen for the tests presented in this paper. As pointed out, target initial suctions used in this experimental program varied between 15 and 100 kPa. However, after consolidation, the suction was allowed to vary and suctions at failure ranged from 2 to 43 kPa.

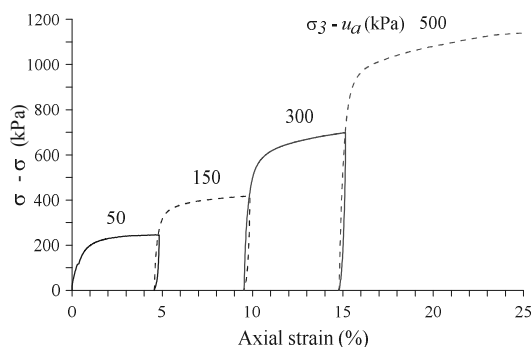


Figure 2. Typical stress-strain curves of the CW tests.

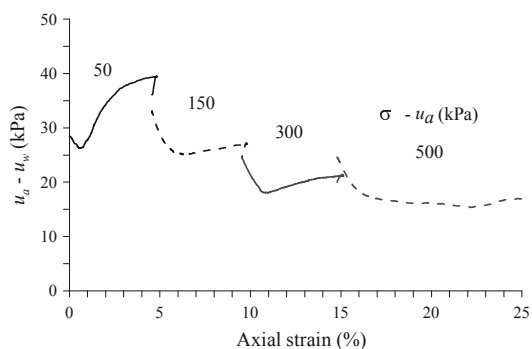


Figure 3. Typical suction changes during shearing of the CW tests.

Data from saturated and unsaturated tests were gathered in the space  $[(\sigma_1 - \sigma_3)/2]$ ,  $[(\sigma_1 + \sigma_3)/2 - u_a]$  and  $(u_a - u_w)$ . Thus, points of maximum ordinates of the Mohr circles and the associated suction at failure were plotted in Figure 4. It is possible to notice that the points are approximately distributed along a plane surface. Taking this into account, the experimental points were fitted by a planar failure surface according to the proposition of Fredlund et al. (1978), resulting into a nice surface fitting with determination coefficient ( $r^2$ ) of 0.99. The obtained shear strength parameters were transferred to the  $\tau$ ,  $(\sigma - u_a)$  and  $(u_a - u_w)$  space, resulting in  $c'$  of 8 kPa,  $\phi'$  of  $32^\circ$  and  $\phi^b$ , the friction angle with respect to suction, equal to  $27^\circ$ . The planar shear strength envelope, expressed in Equation 3, shows an internal friction angle that is quite close to the value derived from the saturated shear strength envelope. The friction angle with respect to suction was lower than  $\phi'$  and the cohesion obtained from the three-dimensional fit was approximately the same value obtained from the saturated envelope.

$$\tau = 8 + (\sigma - u_a) \tan 32^\circ + (u_a - u_w) \tan 27^\circ \quad [\text{kPa}] \quad (3)$$

where  $\tau$  is the shear strength and  $(\sigma - u_a)$  is the net normal stress.

Non-linearity in the relationship between shear strength and soil suction has been recognized by many authors, however this was not evident in this case probably due to the small range of suction registered at failure.

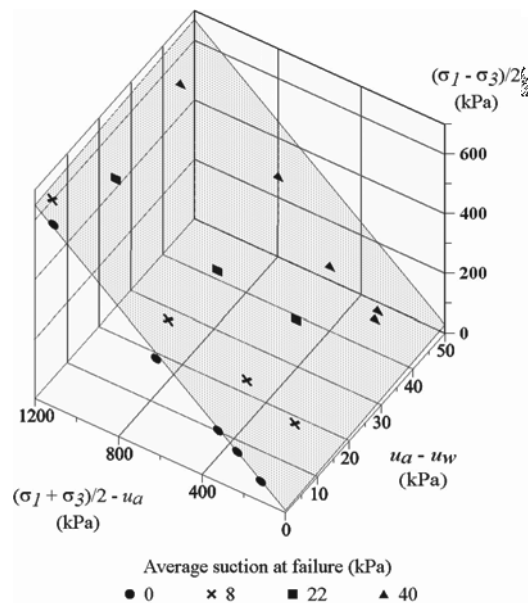


Figure 4. Planar shear strength envelope in the space  $[(\sigma_1 - \sigma_3)/2]$ ,  $[(\sigma_1 + \sigma_3)/2 - u_a]$  and  $(u_a - u_w)$ .

### 3.2. Small-strain shear modulus

From the tests performed with bender elements, the shear wave velocities were calculated and plotted against the wave path length ( $L$ ) to wavelength ( $\lambda$ ) ratios. The wavelength was estimated from the relation between  $V_s$  and the frequency of the input signal. According to Sanchez-Salinerio et al. (1986) and other authors, the  $L/\lambda$  is useful to select signals with reduced near-field effects. An analysis of the results of the saturated and unsaturated bender element tests indicated that the shear wave velocity tended to remain constant when  $L/\lambda$  is larger than 3. Therefore, the wave velocity in each stress condition was taken as the average velocity for  $L/\lambda \geq 3$ .

The influence of isotropic confining stress and suction on the small-strain shear modulus of the soil is shown in Figures 5 and 6. Both figures readily indicate that an increase in any of these variables is able to rise  $G_o$ , which ranged from 78 to 468 MPa. In Figure 5, it can be noticed that potential curves (Equation 4) nicely fitted the experimental data of  $G_o$  versus confining stress. The parameters obtained from the fits can be seen in Table 1.

$$G_o = a(\sigma_3 - u_a)^b \quad (4)$$

where  $G_o$  is in MPa,  $(\sigma_3 - u_a)$  represents either effective or net isotropic stress in kPa, and  $a$  and  $b$  are empirical fitting parameters.

In Table 1, some aspects of the influence of suction on the small-strain shear modulus can be observed. The parameter  $a$  increased with increasing suction. Moreover, the constant  $b$  decreased when suction increased, which means that the net confining stress has more influence on the soil under lower suctions than on the soil under higher suctions.

The small-strain shear modulus variation with suction is shown in Figure 6, where a hyperbolic function (Equation 5) better suited the experimental data in comparison to the potential fit. Table 2 shows the parameters of Equation 5 for each confining stress.

$$G_o = G_{o\text{sat}} + \frac{u_a - u_w}{m + n \cdot (u_a - u_w)} \quad (5)$$

where  $G_{o\text{sat}}$  is the small-strain shear modulus of the saturated soil,  $m$  and  $n$  are empirical fitting parameters,  $G_o$  and  $G_{o\text{sat}}$  are in MPa,  $(u_a - u_w)$  in kPa.

As can be seen, the experimental data is nicely fitted by a non-linear relationship between small-strain shear modulus and the variables suction and confining pressure. The non-linearity between shear modulus and net confining stress or soil suction was also observed for sands by Nyunt et al. (2011) who used, however, different fitting equations to represent these relationships.

The hyperbolic fit suggests that  $G_o$  tends asymptotically to a limit value, which for the range of suction tested, seems to be close to the shear modulus associated to the suction of 100 kPa. However, tests at larger suction should be performed to confirm this behavior.

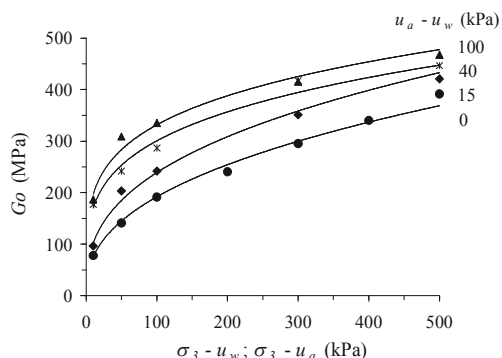


Figure 5. Variation of the small-strain shear modulus with confining stress.

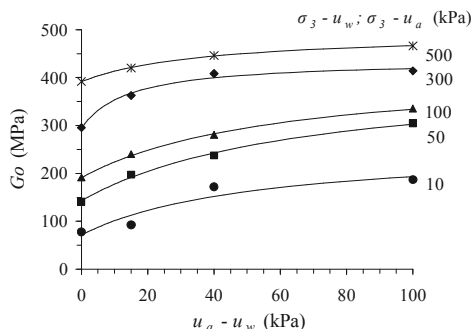


Figure 6. Variation of the small-strain shear modulus with suction.

Table 1. Parameters of the potential fits.

Soil suction	<i>a</i>	<i>b</i>	<i>r</i> <sup>2</sup>
0 kPa (saturated)	29.7	0.406	0.99
15 kPa	43.6	0.369	0.99
40 kPa	96.2	0.247	0.98
100 kPa	116.9	0.227	0.98

Table 2. Parameters of the hyperbolic fits.

Net confining stress (kPa)	$G_{o\ sat}$ (MPa)	<i>m</i>	<i>n</i>	<i>r</i> <sup>2</sup>
10	71.5	0.282	0.0054	0.90
50	142.8	0.251	0.0037	0.99
100	191.0	0.261	0.0044	0.99
300	293.8	0.098	0.0070	0.98
500	391.1	0.357	0.0097	0.99

#### 4 CONCLUSIONS

Triaxial compression and bender element tests were performed on saturated and unsaturated compacted sandy soil. Aiming at reducing the time consumed on unsaturated tests, the specimens went through suction imposition prior to testing and shear strength was measured in multistage constant water content tests.

A planar failure envelope, as suggested by Fredlund et al. (1978), was able to represent shear strength of non-saturated soil, as non-linearity was not evident in the experimental data.

This behavior was probably associated to the small range of soil suction registered at failure, since some non-linearity has been reported in the literature to affect the relationship between shear strength and suction.

The wave path length to wavelength ratio was used to evaluate the interference of near-field effects on the shear wave velocities and resulting shear modulus. The small-strain shear modulus tended to increase non-linearly with net confining stress and soil suction. The increasing of shear modulus with net confining stress was more significant as suction was reduced. The shear modulus has increased with suction, seeming to approach an asymptotic value.

#### 5 ACKNOWLEDGEMENTS

The authors acknowledge CAPES, FAPESP and CNPq (Brazilian Research Agencies) for the financial support given to this research.

#### 6 REFERENCES

Atkinson J.H. and Salfors G. 1991. Experimental determination of stress-strain-time characteristics in laboratory and in situ tests. In *Proc. 10<sup>th</sup> European Conf. Soil Mech. and Found. Eng., Florence, 27-30 May 1991*. Rotterdam: A A Balkema.

Chan C.-M. 2010. Bender element test in soil specimens: identifying the shear wave arrival time. *Electronic Journal of Geotechnical Engineering* 15(M), 1263-1275.

Clayton C.R.I. 2011. Stiffness at small strain: research and practice. *Géotechnique* 61(1), 5-37.

Dyvik R. and Madshus C. 1985. Laboratory measurements of  $G_{max}$  using bender elements. In Khosla V. (ed.) *Proc. Annual Conv. ASCE: Advances in the art of testing soil under cyclic loading, Detroit*. New York: American Society of Civil Engineers.

Fredlund D.G. and Rahardjo H. 1993. *Soil mechanics for unsaturated soils*. New York: John Wiley & Sons, Inc.

Fredlund D.G. and Xing A. 1994. Equations for the soil-water characteristic curve. *Canadian Geotechnical Journal* 31(3), 521-532.

Fredlund D.G., Morgerstern N.R. and Widger R.A. 1978. The shear strength of unsaturated soils. *Canadian Geotechnical Journal* 15(3), 313-321.

Georgetti G.B. and Vilar O.M. 2010. Constant water content triaxial compression tests with a compacted soil. In Alonso E. and Gens A. (eds.) *Proc. 5<sup>th</sup> Intern. Conf. on Unsaturated Soils, Barcelona, 6-8 September, 2010*. London: Taylor & Francis Group.

Hilf J.W. 1956. *An investigation of pore-water pressure in compacted cohesive soils*. PhD Thesis, Faculty of Graduate School of the University of Colorado, Denver.

Ho D.Y.F. and Fredlund D.G. 1982. A multistage triaxial test for unsaturated soils. *Geotechnical Testing Journal* 15(1/2), 18-25.

Hoyos L.R., Takkabutr P., Puppala A.J. and Hossain M.D.S. 2008. Dynamic response of unsaturated soils using resonant column and bender element testing techniques. In Zeng D., Manzari M.T. and Hiltunen D.R. (eds) *Proc. IV Conf. Geotechnical Earthquake Engineering and Soil Dynamics, Sacramento, 18-22 May 2008*. Reston: ASCE.

Jardine R.J., Symes M.J. and Burland J.B. 1984. The measurement of soil stiffness in the triaxial apparatus. *Géotechnique* 34(3), 323-340.

Nyunt T.T., Leong E.C. and Rahardjo H. 2011. Strength and small-strain stiffness characteristics of unsaturated sand. *Geotechnical Testing Journal* 34(5).

Rahardjo H., Heng O.B. and Choon, L.E. 2004. Shear strength of a compacted residual soil from consolidated drained and constant water content triaxial tests. *Canadian Geotechnical Journal* 41, 421-436.

Sanchez-Salinerio I., Roesset J.M. and Stokoe K.H.II. 1986. *Analytical Studies of body wave propagation and attenuation*. Report No. GR 86-15. Austin: Civil Engineering Department, University of Texas at Austin.

Youn J.-U., Choo Y.-W. and Kim D.-S. 2008. Measurement of small-strain shear modulus  $G_{max}$  of dry and saturated sands by bender element, resonant column, and torsional shear tests. *Canadian Geotechnical Journal* 45, 1426-1438.